Biochimica et Biophysica Acta 1818 (2012) 2725–2731

Contents lists available at SciVerse ScienceDirect

Biochimica et Biophysica Acta

journal homepage: www.elsevier.com/locate/bbamem

The DNA–DNA spacing in gemini surfactants–DOPE–DNA complexes

Petra Pullmannová [a,*], Sergio S. Funari [b], Ferdinand Devínsky [c], Daniela Uhríková [a]

[a] Department of Physical Chemistry of Drugs, Faculty of Pharmacy, Comenius University, Odbojárov 10, SK-832 32 Bratislava, Slovakia
[b] HASYLAB at DESY, Notkestr. 85, D-22607 Hamburg, Germany
[c] Department of Chemical Theory of Drugs, Faculty of Pharmacy, Comenius University, Odbojárov 10, SK-832 32 Bratislava, Slovakia

ARTICLE INFO

Article history:
Received 27 September 2011
Received in revised form 10 May 2012
Accepted 18 May 2012
Available online 24 May 2012

Keywords:
DNA
Dioleoylphosphatidylethanolamine
Gemini surfactant
Small angle X-ray diffraction

ABSTRACT

Gemini surfactants from the homologous series of alkane-α,ω-diyl-bis(dodecyldimethylammonium bromide) (CnCS12, number of spacer carbons $n = 2-12$) and dioleoylphosphatidylethanolamine (DOPE) were used for cationic liposome (CL) preparation. CLs condense highly polymerized DNA creating complexes. Small-angle X-ray diffraction identified them as condensed lamellar phase L_α^C in the studied range of molar ratios CnGS12/DOPE in the temperature range 20–60 °C. The DNA–DNA distance (d_{DNA}) is studied in dependence to CnGS12 spacer length and membrane surface charge density. The high membrane surface charge densities (CnGS12/DOPE = 0.35 and 0.4 mol/mol) lead to the linear dependence of d_{DNA} vs. n correlating with the interfacial area of the CnGS12 molecule.

1. Introduction

Gemini surfactants (GS) were synthesized as promising amphiphilic compounds due to their excellent self-assemble properties. They contain two polar headgroups and two aliphatic chains linked by a spacer [1,2]. GS show greatly enhanced surfactant properties relative to the corresponding monomeric (single chain, single head group) compounds—their surface activity can be increased 1000-fold. This makes them interesting for biological and especially biomedical research.

Generally, cationic surfactants can create complexes with polyanions including nucleic acids, giving rise to various periodical structures of great interest for biomedical or industrial applications [3]. For example, DNA–cetyltrimethylammonium bromide–hexanol aggregates express complex phase behavior in dependence on the increasing hexanol content. The addition of hexanol leads to simultaneous lowering of the charge density and bare rigidity of the bilayers. The same effect can, in principle, be independently achieved by adding a neutral lipid [4]. GS carrying a positive charge condense DNA and can act as agent in nucleic acid transfection [5,6] and bacterial transformation [7].

Within this study we focus on the simple type of GS alkane-α,ω-diyl-bis(alkyldimethylammonium bromide) (CnGSm, where $n = 2$–12 is the number of spacer carbons and $m = 12$ is the number of carbons in the alkyl tails) (Fig. 1). The physico-chemical and micellar properties of CnGSm have attracted extensive scientific interest, focusing particularly on the role of the spacer. For example, the critical micelle concentration of homologous series CnGS12 with a hydrophobic polymethylene spacer express a maximum at $n = 4$–6 [8–10]. The surface occupied by one surfactant at air/solution interface reaches a maximum at $n = 10$–12 [10–13]. At $n > 10$ the spacer becomes too hydrophobic to remain in contact with water and adopts a looped (wicket-like) conformation [12].

The CnGSm can interact with DNA either as monomers, micelles [14–17] or as a dispersion of CnGSm–phospholipid liposomes forming complexes with regular inner microstructure [18–20]. Neutral lipid used together with cationic components moderates the structural properties and the membrane surface charge density of the complex. Neutral lipid also facilitates the transport of the complex through the cell's membrane during transfection [21,22]. Several types of CnGSm-phospholipid–DNA complexes arrangement have been observed: condensed lamellar phase L_α^C with ordered DNA monolayers intercalated between lipid bilayers [18,20,23], condensed inverted hexagonal phase H_{II}^C with linear DNA molecules surrounded by lipid monolayers forming inverted cylindrical micelles arranged on a hexagonal lattice [24–26] and also a cubic phase [27] were reported. The membrane surface charge density was found to be a key parameter for the transfection efficiency of L_α^C phase-forming complexes. Lin et al. [28] defines the optimal membrane surface charge density $\sigma_m^* \approx 0.0104\ e^-/Å^2 \approx 1.04\ e^-/1\ nm^2$ for stable complexes allowing successful escape of DNA from the complexes through their fusion with endosomal membranes.

Complexes CnGS12–dioleyphosphatidylethanolamine (DOPE)–DNA have been tested as gene delivery carriers for somatic cells *in vitro* [20]

Abbreviations: A_{CnGS12}, CnGS12 surfactant headgroup area; C12TMA, dodecyltrimethylammonium bromide; CL, cationic liposomes; CnGS12, alkane-α,ω-diyl-bis(dodecyldimethylammonium bromide); DNA, deoxyribonucleic acid; DOPE, dioleoylphosphatidylethanolammine; GS, gemini surfactant; H_{II}^C, condensed inverse hexagonal phase; L_α^C, condensed lamellar phase; R_4N^+, quaternary ammonium group

* Corresponding author. Tel.: +421 250117289.
E-mail address: pullmannova@fpharm.uniba.sk (P. Pullmannová).

0005-2736/$ – see front matter © 2012 Elsevier B.V. All rights reserved.
doi:10.1016/j.bbamem.2012.05.021

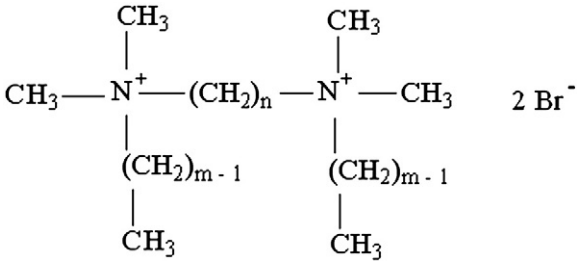

Fig. 1. The scheme of the structure of alkane-α,ω-diyl-bis(dodecyldimethylammonium bromide) molecule (CnCS12, $n=2$–12 is the number of spacer carbons, $m=12$ is the number of alkyl carbons).

and *in vivo* [29]. The character of the spacer has been found to play a role in the transfection efficiency of DNA complexes based on GS [20,30,31]. The highest transfection activity *in vitro* was detected at CnGSm compounds having the spacer of three carbons (C3GS12, C3GS16) [20]. Generally, GS with short spacer length were reported regarding their enhanced transfection activity. For example C2GS14/cholesterol/DOPE = 2:1:1 mol/mol/mol [32] and derivatives of *N,N*-bisdimethyl-1,2-ethanediamine with 2 carbons in the spacer and 12 carbons in alkyl chains, in a mixture with DOPE (1:2 mol/mol) have shown significantly higher tranfection activity in comparison to a standard commercial transfection reagent [33].

In spite of published results in transfection efficiency of CnGSm–neutral phospholipid carriers for DNA, information about the particle's microstructure, their polymorphic behavior and the role of CnGSm spacer length in DNA packing is rather scarce in literature. We used small-angle X-ray diffraction (SAXD) to study the microstructure of complexes formed due to DNA interaction with cationic liposomes (CL) prepared as a mixture of CnGS12 with various spacer $n=2$–12 and DOPE. In this study we focus our attention on a role of the spacer's length in the DNA packing in L_α^C phase.

2. Materials and methods

DOPE (1,2-dioleoyl-*sn*-glycero-3-phosphoethanolamine) was obtained from Avanti Polar Lipids, Inc., USA; highly polymerized calf thymus deoxyribonucleic acid (sodium salt) type I (DNA, average Mr of nucleotide 308) from Sigma Chemicals Co., USA. Alkane-α,ω-diyl-bis(dodecyldimethylammonium bromide) (CnCS12, number of spacer carbons $n=2$–12) were prepared as described in ref. [1] and purified by manyfold crystallization from a mixture of acetone and methanol. Dodecyltrimethylammonium bromide (C12TMA) was purchased from Fluka Chemie AG, Buchs, Switzerland. Sodium chloride (NaCl) was obtained from Lachema, Brno, Czech Republic. The chemicals were of analytical grade and were used without further purification. The aqueous solution of NaCl was prepared with redistilled water, pH ~ 6, at concentration 150 mM. The solution of DNA was prepared by dissolving DNA in 150 mM NaCl solution, the precise value of DNA concentration was determined spectrophotometrically (Hewlett Packard 8452A Diode array spectrophotometer), according to: $c_{DNA}=A_{260}.\ 47\times10^{-6}$ [g/ml], where A_{260} is the absorbance at wavelength $\lambda=260$ nm. The concentration of DNA is referred as molar concentration of DNA base pairs (mol bp). The purity of DNA was checked by measuring the absorbance A_λ at $\lambda=260$, 230 and 280 nm. We have obtained the values of $A_{260}/A_{230}=2.23$ and $A_{260}/A_{280}=1.76$. DOPE, CnGS12 and C12TMA were dissolved in organic solvent (mixture of chloroform and methanol at volume ratio = 3:1). The appropriate amounts of organic stock solutions were added to obtain a lipid mixture with the desired ratio cationic surfactant/DOPE. The solvent was evaporated under a stream of gaseous nitrogen and its residue removed by vacuum. The dry mixture was hydrated by 150 mM NaCl solution for 12 hours and afterwards homogenized (by vortexing, freezing-thawing cycles or sonication in ultrasound bath) until an opalescent liposome dispersion was created. A fully hydrated DOPE was used as a control sample.

The samples were prepared at the calculated isoelectric point CnCS12/DNA = 1 [mol/mol bp]. The DNA solution was added to the liposome dispersion at once and the sample was shortly mixed. A precipitate was created spontaneously during the mixing. To exclude the possibility of an incomplete binding of DNA in DNA–CL, we measured the residual DNA concentration in the sample's supernatant spectrophotometrically for CnGS12–DOPE–DNA and C12TMA–DOPE–DNA complexes. The average DNA condensation efficiency was 98.1 ± 1.9% reporting to an effective binding of DNA. The samples were stored at 2–6 °C or in a freezer at approx. −20 °C.

Before the measurement the samples were shortly centrifuged. The sedimented precipitate with a few drops of bulk solution was enclosed between two Kapton (Dupont, France) windows of a sample holder for X-ray diffraction. Small- (SAXD) and wide-angle (WAXD) synchrotron radiation diffraction experiments were performed at the soft condensed matter beamline A2 at HASYLAB at the Deutsches Elektronen Synchrotron (DESY) in Hamburg (Germany), using a monochromatic radiation of wavelength $\lambda=0.15$ nm. The sample was equilibrated at selected temperature (20 or 60 °C) before exposure to radiation. The evacuated double-focusing camera was equipped with a linear position sensitive detector for WAXD and a 2D MarCCD detector or a linear position sensitive detector for SAXD. The raw data were normalized against the incident beam intensity. The SAXD patterns were calibrated using Ag behenate [34] or rat tail collagen [35] and the WAXD patterns by tripalmitin or polyethylene terephthalate [36,37]. Each diffraction peak of SAXD region was fitted with a Lorentzian above a linear background using the Origin software. The WAXD pattern of all measured samples exhibited one wide diffuse scattering in the range $s\sim1.8$–$3.2\ nm^{-1}$, characteristic for liquid-like carbon chains of phospholipid and CnGS12 molecules. We do not show WAXD patterns because we observed no qualitative change in WAXD patterns in the temperature range 20–60°.

3. Results and discussion

3.1. The effect of surface charge density

The structure of complexes C3GS12–DOPE–DNA was investigated throughout the range of molar ratios $0.1\le$ C3GS12/DOPE ≤0.5 mol/mol (at 20 °C). We determined the structural parameters of complexes with the aim to find out the appropriate range of molar ratios to study the spacer's effect. Representative SAXD patterns are shown in Fig. 2A. At the molar ratios C3GS12/DOPE ≥0.15 we observed two sharp reflections L(1) and L(2) having the origin in a lamellar structure of lipid bilayers. The repeat distance d was evaluated as $d=1/s_1$, where s_1 is the first order reflection's maximum. The DNA exhibits a broad small peak at $s_{DNA}=1/d_{DNA}$, where d_{DNA} is the average distance of periodically spaced DNA strands. The repeat distance d involves the thickness of phospholipids bilayer d_L and the water thickness containing a monolayer of hydrated DNA strands d_W, so $d=d_L+d_W$. The thickness of hydrated DNA monolayer d_W is assumed to be not less than $d_W\sim2.45$ nm [38]. The observed SAXD patterns are typical for a condensed lamellar phase L_α^C of complexes DNA–CL. At low molar ratios C3GS12/DOPE ≤0.12, the coexistence of L_α^C phase and condensed hexagonal phase H_{II}^C is observed. We have shown earlier [26], that the heating of complexes CnGS12–DOPE–DNA leads to the increase in the fraction of H_{II}^C phase due to a phase transition $L_\alpha^C\rightarrow H_{II}^C$. The lattice parameter of the H_{II}^C phase in complexes at C3GS12/DOPE = 0.12 mol/mol is $a=2/\sqrt{3}\,s_1^{'}=7.14$ nm, where $s_1^{'}$ is the first order reflection's maximum of H_{II}^C phase. The fully hydrated DOPE used as a control sample formed an inverted hexagonal phase H_{II} with the lattice parameter $a=7.58$ nm (at 20 °C). DOPE has an inverted truncated cone-shaped molecule and confers a negative spontaneous curvature to membranes. Although hydrated DOPE forms inverted hexagonal phase, the sufficient content of C3GS12 surfactant stabilizes the

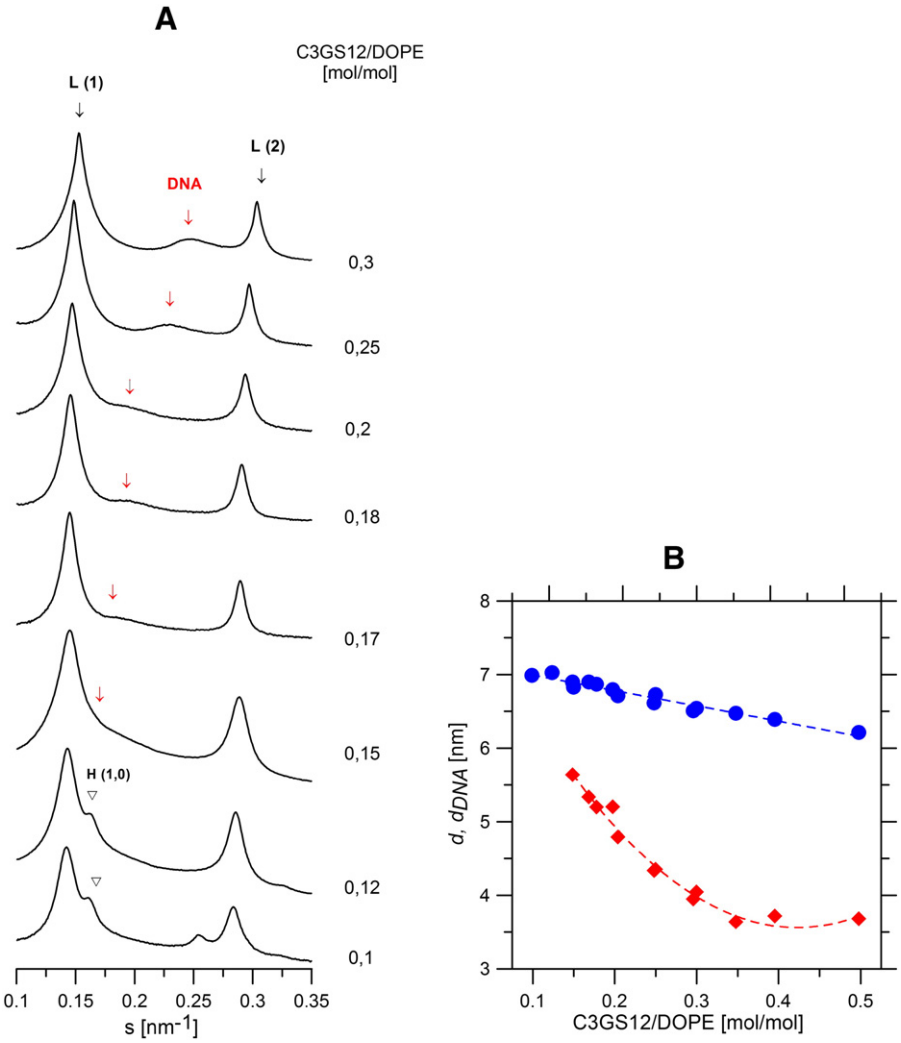

Fig. 2. (A) Representative SAXD patterns of C3GS12–DOPE–DNA complexes at various molar ratio C3GS12/DOPE at 20 °C. The relative intensity is in logarithmic scale. The 1st reflection maxima of H_{II}^{C} phase are marked by triangles. (B) The repeat distance d (●) [nm] and DNA interhelical distance d_{DNA} (◆) [nm] *vs.* molar ratio C3GS12/DOPE in complexes C3GS12-DOPE-DNA at 20 °C. The dashed lines are only guidelines.

lamellar arrangement of lipid bilayers within the complexes C3GS12–DOPE–DNA. At 20 °C, the molar ratio C3GS12/DOPE = 0.15 mol/mol represents the lowest limit for the stable L_{α}^{C} phase of complexes.

The structural parameters d and d_{DNA} of the C3GS12-DOPE-DNA complexes are shown in Fig. 2B. The repeat distance d decreases linearly with increasing molar ratio C3GS12/DOPE. The DNA interhelical distance d_{DNA} decreases non-linearly with increasing molar ratio up to C3GS12/DOPE = 0.35 mol/mol. Further increase of C3GS12 fraction within the lipid mixture did not change d_{DNA} significantly. The effective surface charge density of membrane, provided by CnGS12 in our experiment, is responsible for d_{DNA} distance, as proven in [39]. The average spacing d_{DNA} between the DNA strands in an isoelectric complex can be expressed in terms of the average anionic charge/length of DNA λ and cationic charge/area of lipid σ_m within the DNA–CL complex [39]:

$$d_{DNA} = \frac{\lambda}{\sigma_m} \quad (1)$$

The d_{DNA} is directly proportional to the average cross-sectional area per lipid molecule in the membrane and inversely proportional to the mole fraction of the cationic content in the lipid mixture [40]. The SAXD peak related to DNA–DNA packing is rather broad and its amplitude is weaker in comparison to the peaks corresponding to the lipid bilayer stacking (discussed thoroughly in [41]). It is evident (Fig. 2) that the C3GS12 molar fraction determines its position. At low C3GS12 fraction (C3GS12/DOPE = 0.15), the position of DNA reflection coincides with the 1st reflection maximum of lipid arrangement, and deconvolution of peaks brings an uncertainty into the analysis. At the high molar ratios C3GS12/DOPE ≥ 0.4 the DNA–DNA spacing does not respond significantly to the C3GS12 fraction changes. Based on these experimental data, we have selected the suitable range of molar ratios 0.2 < CnGS12/DOPE < 0.4 to follow the effect of the CnGS12 spacer length on DNA–DNA packing.

3.2. The effect of the spacer on d_{DNA} at molar ratio CnGS12/DOPE = 0.3

We started to study the effect of n at the intermediate molar ratio CnGS12/DOPE = 0.3. Complexes with monoalkylammonium bromide C12TMA were used as a reference model for charged surfactant molecules freely distributed in the membrane surface. The SAXD patterns of the CnGS12–DOPE–DNA and C12TMA–DOPE–DNA complexes at 20 °C are shown in Fig. 3A, where CnGS12/DOPE = 0.3; C12TMA/DOPE = 0.6 mol/mol. In both cases the ratio between cationic quaternary ammonium group and DOPE (R_4N^+/DOPE) is the same 0.6 mol/mol. At the chosen molar ratios, all studied complexes have shown L_{α}^{C} phase up to 60 °C (Supplementary material, Fig. 6sA).

The structural parameters d and d_{DNA} as a function of the number of spacer carbons n are shown in Fig. 3B. The experiment was repeated

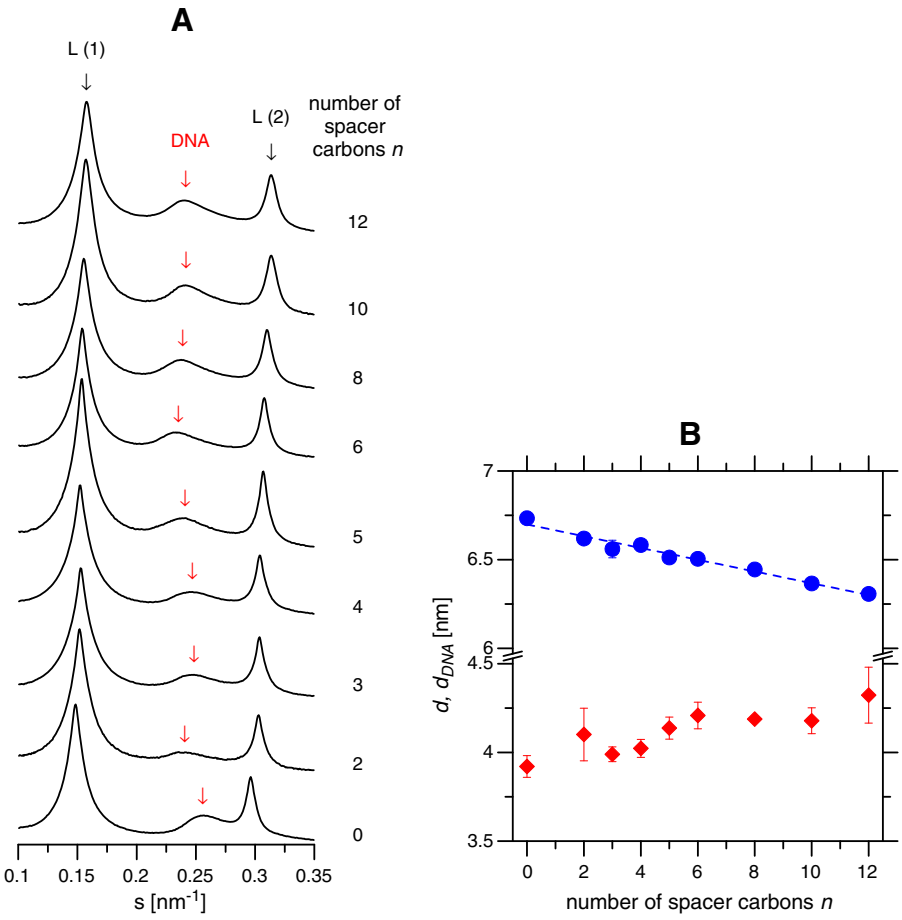

Fig. 3. (A) SAXD patterns of CnGS12–DOPE–DNA and C12TMA–DOPE–DNA complexes at molar ratio CnGS12/DOPE = 0.3 and C12TMA/DOPE = 0.6 at 20 °C. The relative intensity is in logarithmic scale. (B) The repeat distance d (●) [nm] and DNA interhelical distance d_{DNA} (♦) [nm] *vs.* number of spacer carbons n in complexes CnGS12–DOPE–DNA and C12TMA–DOPE–DNA at 20 °C; $n = 0$ for the complex containing C12TMA. The molar ratio CnGS12/DOPE = 0.3 and C12TMA/DOPE = 0.6. Each point represents the average of separate determinations, and the vertical bars on each point indicate the standard deviation for data of independent experiments.

three times. The d and d_{DNA} values in Fig. 3B represent the average values and error bars represent the standard deviations. For C12TMA–DOPE–DNA complexes we adapted $n = 0$.

With increasing n, the lamellar periodicity d linearly decreases from 6.73 nm at $n = 0$ to 6.31 nm at $n = 12$ (at 20 °C). Complexes were heated to 60 °C, where the repeat distance d has attained the values in the range from 6.52 nm at $n = 0$ to ~6.2 nm at $n = 10$ and 12 (Supplementary material, Fig. 6sB). The repeat distance d decreases with the increase of the temperature in all complexes. The decrease of d of L_α^C phase can be induced either by the higher temperature or by the addition of higher fraction of CnGS12 into the phospholipids bilayer, as determined in the Fig. 2B. Generally, both factors induce a lateral expansion of the membrane linked with a decrease of the lipid bilayer thickness and a decrease of the hydration level of hydrophilic segments [42–44]. The increasing number of spacer carbons n also resulted in a decrease of the repeat distance d. The spacer's elongation probably causes the reduction of L_α^C repeat distance d due to the lateral membrane expansion and/or the changes in the hydrophilic region hydration.

As is evident in the Fig. 3B, the DNA–DNA interhelical distance d_{DNA} slightly increases with the increasing number of spacer carbons n. We have found the smallest value of $d_{DNA} = 3.92 \pm 0.06$ nm in complexes with C12TMA monoalkylammonium surfactant and the maximum at $n = 12$ is equal to $d_{DNA} = 4.32 \pm 0.16$ nm. However, the detailed inspection of the dependence d_{DNA} *vs.* n in Fig. 3B shows small deviations from the linear character (namely at the $n = 3$ and 10). At 60 °C, the d_{DNA} *vs.* n dependence has shown similar course with d_{DNA} slightly shifted to higher values (d_{DNA} changed from 4.15 nm at $n = 0$ to 4.42 nm at $n = 12$) due to thermally induced lateral expansion of the membrane (Supplementary material, Fig. 6sB). The changes of d_{DNA} in the DNA–CL complexes significantly depend on the increasing n. The spacer length affects the spatial arrangement of the lipid membrane and the resulting membrane surface charge density. The simplest explanation of the spacer effect would be that those changes of the membrane rise due to the increase of the CnGS12 headgroup area as the spacer elongates. The bigger headgroup area of CnGS12 with longer spacer leads to the lower membrane surface charge density σ_m (expressed as the charge per surface area). Consequently the d_{DNA} increases. However, the relationship between number of spacer carbons n and d_{DNA} is not simply linear. Several other factors must participate in the effect of various n on the DNA arrangement.

3.3. The effect of spacer on d_{DNA} at various molar ratios CnGS12/DOPE

The non-linear dependence d_{DNA} vs. n led us to test the role of spacer in DNA arrangement at different surface charge densities. We prepared three series of samples at different molar ratios R_4N^+/DOPE = 0.5, 0.7 and 0.8. All complexes have shown the condensed lamellar phase L_α^C at 20 °C. The repeat distance d decreases with increasing number of spacer carbons n in the all cases (Supplementary material, Fig. 7s). While at molar ratios R_4N^+/DOPE = 0.7 and 0.8 the dependence of d *vs.* n has a linear character (R^2 ~ 0.91–0.98), at R_4N^+/DOPE = 0.5 anomalies are present in the dependence.

The dependences of d_{DNA} vs. n for the discussed molar ratios R_4N^+/DOPE are plotted in Fig. 4. At the low molar ratio R_4N^+/DOPE = 0.5, we observe a non-linear course of d_{DNA} vs. n. The d_{DNA} values are considerably higher in comparison with those at the high molar ratios R_4N^+/

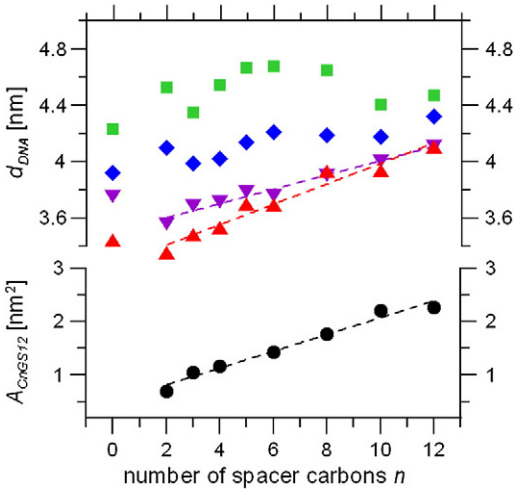

Fig. 4. The DNA interhelical distance d_{DNA} [nm] vs. number of spacer carbons n at the molar ratios CnGS12/DOPE = 0.4 and C12TMA/DOPE = 0.8 (▲); CnGS12/DOPE = 0.35 and C12TMA/DOPE = 0.7 (▼); CnGS12/DOPE = 0.3 and C12TMA/DOPE = 0.6 (♦); CnGS12/DOPE = 0.25 and C12TMA/DOPE = 0.5 (■) at 20 °C; the headgroup area *vs.* number of spacer carbons n (●), adapted from [11,12]; $n = 0$ for the complex containing C12TMA. The dashed lines represent linear fits.

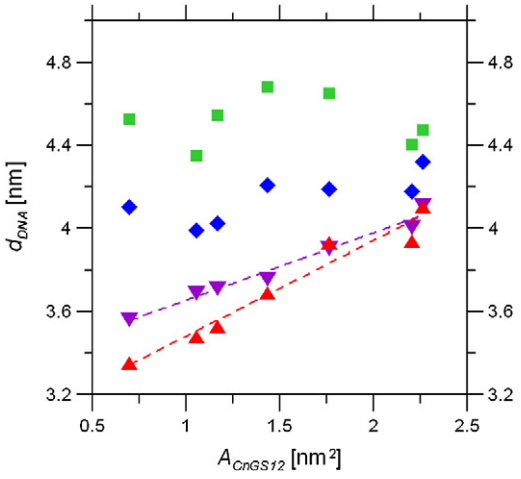

Fig. 5. The DNA interhelical distance d_{DNA} [nm] vs. the headgroup area adopted from [11,12]; at molar ratios CnGS12/DOPE = 0.4 (▲); CnGS12/DOPE = 0.35 (▼); CnGS12/DOPE = 0.3 (♦) and CnGS12/DOPE = 0.25 (■). The dashed lines represent linear fits.

DOPE. At the high molar ratios R_4N^+/DOPE = 0.7 and 0.8 the course of the d_{DNA} vs. n dependence is linear for $n = 2$–12 (Fig. 4) and the best-fitting lines to data differ in the slope. The d_{DNA} values converge at R_4N^+/DOPE = 0.7 and 0.8 with increasing n. The molar ratio R_4N^+/DOPE = 0.8 lays on the upper bound of the appropriate molar ratio's interval estimated from Fig. 2B. That can be the reason why d_{DNA} does not change significantly for CnGS12 with $n \geq 6$ when the molar ratio R_4N^+/DOPE increases from 0.7 to 0.8. Fig. 4 shows also the dependence of CnGS12 headgroup area (A_{CnGS12}) as a function of n having linear character. The values of A_{CnGS12} were adopted from refs. [11,12], determined for CnGS12 molecules at water/air interface. The A_{CnGS12} are in excellent agreement with data published in [10] and correlate with [13]. Both our dependences d_{DNA} vs. n at high molar ratios correlate with the dependence of A_{CnGS12} vs. n.

Comparing the effect of CnGS12 and C12TMA molecules, we have found that $d_{DNA(C12TMA)} < d_{DNA\ (CnGS12)}$ (indices are related to the representative surfactant) at molar ratios R_4N^+/DOPE = 0.5 and 0.6. At the high molar ratios R_4N^+/DOPE = 0.7 and 0.8, $d_{DNA\ (C12TMA)} \geq d_{DNA\ (CnGS12)}$ at $n \leq 6$ and at $n \leq 2$, respectively.

In Fig. 5 we summarize the d_{DNA} values of CnGS12–DOPE–DNA complexes at all studied molar ratios as a function of A_{CnGS12}. At the high molar ratios R_4N^+/DOPE = 0.7 and 0.8, we fitted d_{DNA} vs. A_{CnGS12} by straight lines ($R^2 \sim 0.95$–0.98) what indicates a good correlation between DNA–DNA packing and the area per CnGS12 molecule for individual length of spacer ($n = 2$–12).

3.4. Discussion

In our experiment, CnGS12 molecules are inserted in DOPE phospholipid bilayer, i.e. the membrane represents a two-components system. Nuclear magnetic resonance studies have revealed the influence of electric surface charge on P^-–N^+ dipole of the phospholipid headgroup in a zwitterionic phosphocholine-cationic surfactant system. As a consequence of P^-–N^+ dipole reorientation, the decrease of the surface lipid area was reported [45,46]. The reorientation of the P^-–N^+ dipole was enhanced in the system with DNA molecules condensed with cationic liposomes [47,48]. The mentioned effect of cationic surfactant to phospholipid headgroup is referred as "stitching" in the experiment with the supported phospholipid bilayers [49]. The experimental data are in agreement with the theoretical studies [50,51].

The obtained correlation d_{DNA} vs. n indicates that at the high molar ratio R_4N^+/DOPE the partial area per CnGS12–DOPE follows simple proportional addition of areas per 1 molecule of both components. Because of steric and electrostatic interactions between charged R_4N^+ and P^-–N^+ dipole of the phospholipid headgroup, the last assumption is rather strong, however frequently used in systems DNA–cationic liposomes forming L_α^C, for example in calculation of membrane surface charge density [20,28,39,52]. To the best of our knowledge, any data related to the membrane surface area of species in phosphatidylethanolamine–cationic surfactant mixture have not been reported so far. Because of that, we will discuss the obtained structural characteristics of CnGS12–DOPE–DNA complexes in view of the relative changes occurring due to the elongation of the polymethylene spacer.

Theoretical models of L_α^C phase assume DNA as "stiff rods" with uniform distribution of negative charge, justified in view of the fact that the persistence length of double-stranded DNA, (~50 nm), is much larger than its ~2 nm diameter [53] and also much larger comparable to membrane dimensions (both, the thicknesses of the lipid bilayer and water layer) [54]. Natural tendency for the charge screening of both, cationic headgroup of CnGS12 and DNA leads to an energetically favorable organization. As we observe in Fig. 2A, the DNA–CL system with the low content of C3GS12 forms the coexisting condensed lamellar–condensed inverse hexagonal phases. The theoretical analysis of systems containing DNA, cationic lipids, and nonionic (helper) lipids revealed that the phase behavior, in particular the preferred lipid-DNA complex geometry, is governed by a subtle interplay between the electrostatic, elastic, and mixing terms, which depend, in turn, on the lipid composition and lipid/DNA ratio. The "soft" membranes with low bending modulus exhibit the formation of both lamellar and hexagonal complexes, sometimes coexisting with each other [40]. The increase of the microviscosity of the phosphocholine membrane caused by added cationic surfactant has been proven also experimentally [55]. The L_α^C and H_{II}^C coexistence at low molar ratio C3GS12/DOPE reflects the low membrane rigidity and tendency to adopt negative curvature of the membrane. The DNA and cationic lipid membrane tend to compensate their charge as effectively as possible, using the entire accessible membrane surface. H_{II}^C phase minimizes the charge separation between the anionic groups on the DNA chain and the cationic lipids. Reduction in the elastic energy barrier allows the preferential forming of H_{II}^C phase, which is favored by the electrostatic interactions [56].

DNA–CL complexes with high surface charge density form L_α^C phase with DNA incorporated between lipid membranes. The DNA strands distribution in L_α^C phase represents one-dimensional smectic phase. Energetically favorable DNA–DNA distance reflects the surface charge density of the membrane. On the other hand, too tight arrangement of the DNA strands is accompanied with the rise of the hydration repulsion between them [39]. The hydration repulsion is

assumed to be a force restricting the DNA strands to get nearer. The hydration repulsion forces dominate the interaction between polar biopolymers at surface separations less than 1.0–1.5 nm [57], what corresponds to the DNA strands separation 3.2–3.5 nm [38]. As we mentioned above, in the region R_4N^+/DOPE ≥ 0.8 a "plateau" was observed in the dependence d_{DNA} *vs.* n of C3GS12–DOPE–DNA complexes (Fig. 2B). In this region d_{DNA} approaches the values relevant for the occurrence of the hydration repulsion.

At the low molar ratios R_4N^+/DOPE = 0.5 and 0.6 the dependence d_{DNA} vs. n express a non-linear character with the lowest value of d_{DNA} in the complexes C12TMA–DOPE–DNA, containing the cationic moieties freely distributed in the membrane (Fig. 4). The DNA strands in complexes without restriction given by the spacer favor the tighter organization, in comparison with those where the spacer's effect is present. Moreover, the d_{DNA} distance in complexes based on CnGS12 changes non-linearly with n. The natural tendency of the complex to come to the energetically optimal organization could be the driving force, which modulates the d_{DNA} distance at various spacer lengths. At the low molar ratio R_4N^+/DOPE complexes tend to minimize the d_{DNA} distance and to reach more tight complex arrangement. From this point of view, the spacer seems to be a barrier in this effort. The actual length of spacer is determined not only by the nominal n, but also by its flexibility and adopted conformation. The distance between cationic moieties of short spacer ($n = 2, 3$) is fixed, whereas the longer spacer at $n = 10–12$ is flexible as well as hydrophobic enough to fold into the lipophilic phase at the interface [12,13]. Thus, the adopted CnGS12 molecule conformation can affect the spatial arrangement of the cationic moieties in the membrane. In the case, that the complex tends to form the tight packing of DNA, the changes of CnGS12 molecule conformation leading to the higher surface charge density would be favored. The flexible long spacers can decrease the distance of cationic headgroups by adopting a suitable looped-like conformation. Because each CnGS12 surfactant differs in the ability to adopt various conformations, the ability to modulate d_{DNA} distance varies also. Finally we observe a non-linear dependence of d_{DNA} vs. n at the conditions of low molar ratios R_4N^+/DOPE.

Reversely, at the high molar ratios R_4N^+/DOPE, the dependence d_{DNA} vs. n has a linear character for $n = 2–12$, where the smallest value d_{DNA} is attained in the complex containing the surfactant with the shortest spacer C2GS12. The DNA strands spread out more in C12TMA–DOPE–DNA complexes, probably due to the hydration repulsion between them. The favorable DNA spacing in C12TMA–DOPE–DNA complexes without the presence of spacer does not represent a minimal value of d_{DNA} in the series. The CnGS12–DOPE–DNA complexes tend to organize itself in the way to attain the optimal DNA–DNA distance and to avoid a too tight arrangement. Thus, a large membrane surface area of CnGS12 would be desirable. In the effort to extend the distance between cationic moieties, the spacer length is a limiting factor. The all-trans conformation of CnGS12 spacer chain maximizes the distance between cationic headgroups and the molecular area A_{CnGS12} manifested on the membrane surface. Moreover, the high fraction of CnGS12 within the lipid membrane can act as a limitation for the mobility of cationic headgroups and surface charge density variation. Under the conditions of the sufficiently high molar ratios R_4N^+/DOPE, the resulting dependence of d_{DNA} vs. n is linear and correlates with A_{CnGS12}, which probably play a main role in the structural arrangement of the complexes. The various flexibility and conformational properties of the spacer become more protracted at lower molar ratios R_4N^+/DOPE, under the tendency to achieve the optimal DNA–DNA distance.

4. Conclusions

We have shown that CnGS12–DOPE–DNA complexes form L_α^C phase with regularly spaced DNA strands having average distance d_{DNA}. The presence and length of the spacer in CnGS12 surfactant molecule affected the structure of complexes and DNA–DNA spacing. The d_{DNA} correlated with the area of CnGS12 surfactant A_{CnGS12} and increased linearly with increasing n at the high studied membrane surface charge densities of the complexes CnGS12/DOPE = 0.35 and 0.4 mol/mol. Lower membrane surface charge densities disrupt the correlation d_{DNA} vs. A_{CnGS12}. The low membrane surface charge densities, i.e. a lack of charged molecules per unit lipid membrane area, facilitate the modulation of d_{DNA} probably due to conformational variability of CnGS12 molecules.

Acknowledgments

Authors thank Department of Physical Chemistry, Faculty of Chemical and Food Technology, Slovak University of Technology, Bratislava, Slovakia for support during the manuscript preparation, Prof. P. Balgavý for fruitful discussion and Doc. I. Lacko for kindly providing the CnGS12 chemicals. Financial support provided by the European Community's Seventh Framework Program (FP7/2007-2013) under grant agreement no 226716 (HASYLAB project II-20100372 EC), by the JINR project 07-4-1069-09/2011, by the VEGA grants 1/0292/09 and 1/1224/12 is gratefully acknowledged.

Appendix A. Supplementary data

Supplementary data to this article can be found online at http://dx.doi.org/10.1016/j.bbamem.2012.05.021.

References

[1] T. Imam, F. Devínsky, I. Lacko, D. Mlynarčík, L. Krasnec, Preparation and antimicrobial activity of some new bisquaternary ammonium salts, Pharmazie 38 (1983) 308–310.
[2] F.M. Menger, C.A. Littau, Gemini-surfactants: synthesis and properties, J. Am. Chem. Soc. 113 (1991) 1451–1452.
[3] R. Krishnaswamy, P. Mitra, V.A. Raghunathan, A.K. Sood, Tuning the structure of surfactant complexes with DNA and other polyelectrolytes, Europhys. Lett. 62 (2003) 357–362.
[4] R. Krishnaswamy, V.A. Raghunathan, A.K. Sood, Reentrant phase transitions of DNA–surfactant complexes, Phys. Rev. E Stat. Nonlinear Soft Matter Phys. 69 (2004) 031905.
[5] A.J. Kirby, P. Camilleri, J.B.F.N. Engberts, M.C. Feiters, R.J.M. Nolte, O. Söderman, M. Bergsma, P.C. Bell, M.L. Fielden, C.L. García Rodríguez, P. Guédat, A. Kremer, C. McGregor, C. Perrin, G. Ronsin, M.C.P. van Eijk, Gemini surfactants: new synthetic vectors for gene transfection, Angew. Chem. Int. Ed Engl. 42 (2003) 1448–1457.
[6] A.D. Miller, Cationic liposomes for gene therapy, Angew. Chem. Int. Ed. 37 (1998) 1768–1785.
[7] L. Horniak, F. Devínsky, P. Balgavý, I. Lacko, L. Ebringer, Quaternary ammonium halides for increased efficiency of bacterial transformation, Patent 88/3,560(CS 269,549), 1990.
[8] F. Devínsky, I. Lacko, T. Imam, Relationship between structure and solubilization properties of some bisquaternary ammonium amphiphiles, J. Colloid Interface Sci. 143 (1991) 336–342.
[9] R. Zana, M. Benrraou, R. Rueff, Alkanediyl- alpha, omega-bis (dimethylalkylammonium bromide) surfactants 1 Effect of the spacer chain length on the critical micelle concentration and micelle ionization degree, Langmuir 7 (1991) 1072–1075.
[10] S.D. Wettig, R.E. Verrall, Thermodynamic studies of aqueous m-s-m gemini surfactant systems, J. Colloid Interface Sci. 235 (2001) 310–316.
[11] A. Espert, R.V. Klitzing, P. Poulin, A. Colin, R. Zana, D. Langevin, Behavior of soap films stabilized by a cationic dimeric surfactant, Langmuir 14 (1998) 4251–4260.
[12] E. Alami, G. Beinert, P. Marie, R. Zana, Alkanediyl-alpha, omega-bis(dimethylalkylammonium bromide) surfactants 3 Behavior at the air-water interface, Langmuir 9 (1993) 1465–1467.
[13] M. Pisárčik, M.J. Rosen, M. Polakovičová, F. Devínsky, I. Lacko, Area per surfactant molecule values of gemini surfactants at the liquid–hydrophobic solid interface, J. Colloid Interface Sci. 289 (2005) 560–565.
[14] X. Zhao, Y. Shang, H. Liu, Y. Hu, Complexation of DNA with cationic gemini surfactant in aqueous solution, J. Colloid Interface Sci. 314 (2007) 478–483.
[15] C. Wang, X. Li, S.D. Wettig, I. Badea, M. Foldvari, R.E. Verrall, Investigation of complexes formed by interaction of cationic gemini surfactants with deoxyribonucleic acid, Phys. Chem. Chem. Phys. 9 (2007) 1616–1628.
[16] D. Uhríková, I. Zajac, M. Dubničková, M. Pisárčik, S.S. Funari, G. Rapp, P. Balgavý, Interaction of gemini surfactants butane-1,4-diyl-bis(alkyldimethylammonium bromide) with DNA, Colloids Surf. B Biointerfaces 42 (2005) 59–68.
[17] L. Karlsson, M.C.P. van Eijk, O. Söderman, Compaction of DNA by gemini surfactants: effects of surfactant architecture, J. Colloid Interface Sci. 252 (2002) 290–296.
[18] D. Uhríková, G. Rapp, P. Balgavý, Condensed lamellar phase in ternary DNA–DLPC–cationic gemini surfactant system: a small-angle synchrotron X-ray diffraction study, Bioelectrochemistry 58 (2002) 87–95.

[19] D. Uhríková, M. Hanulová, S.S. Funari, I. Lacko, F. Devínsky, P. Balgavý, The structure of DNA–DLPC–cationic gemini surfactant aggregates: a small angle synchrotron X-ray diffraction study, Biophys. Chem. 111 (2004) 197–204.
[20] M. Foldvari, I. Badea, S. Wettig, R. Verrall, M. Bagonluri, Structural characterization of novel gemini non-viral DNA delivery systems for cutaneous gene therapy, J. Exp. Nanosci. 1 (2006) 165–176.
[21] D. Hirsch-Lerner, M. Zhang, H. Eliyahu, M.E. Ferrari, C.J. Wheeler, Y. Barenholz, Effect of "helper lipid" on lipoplex electrostatics, Biochim. Biophys. Acta 1714 (2005) 71–84.
[22] R. Koynova, L. Wang, Y. Tarahovsky, R.C. MacDonald, Lipid phase control of DNA delivery, Bioconjug. Chem. 16 (2005) 1335–1339.
[23] S.D. Wettig, I. Badea, M. Donkuru, R.E. Verrall, M. Foldvari, Structural and transfection properties of amine-substituted gemini surfactant-based nanoparticles, J. Gene Med. 9 (2007) 649–658.
[24] S.D. Wettig, R.E. Verrall, M. Foldvari, Gemini surfactants: a new family of building blocks for non-viral gene delivery systems, Curr. Gene Ther. 8 (2008) 9–23.
[25] D. Uhríková, A. Šabíková, M. Hanulová, S.S. Funari, I. Lacko, F. Devínsky, The microstructure of DNA–EYPC–gemini surfactants aggregates: a small angle X-ray diffraction study, Acta Facult. Pharm. Univ. Comenianae 54 (2007) 198–208.
[26] P. Pullmannová, D. Uhríkova, S.S. Funari, I. Lacko, F. Devínsky, P. Balgavý, Polymorphic phase behavior of DNA–DOPE–Gemini surfactant aggregates: a small angle X-ray diffraction, Acta Facult. Pharm. Univ. Comenianae 55 (2008) 170–182.
[27] M. Foldvari, S. Wettig, I. Badea, R. Verrall, M. Bagonluri, Dicationic gemini surfactant gene delivery complexes contain cubic-lamellar mixed polymorphic phase, 2006 NSTI Nanotechnology Conference and Trade Show - NSTI Nanotech 2006 Technical Proceedings, 2006, pp. 400–403.
[28] A.J. Lin, N.L. Slack, A. Ahmad, C.X. George, C.E. Samuel, C.R. Safinya, Three-dimensional imaging of lipid gene-carriers: membrane charge density controls universal transfection behavior in lamellar cationic liposome-DNA complexes, Biophys. J. 84 (2003) 3307–3316.
[29] I. Badea, R. Verrall, M. Baca-Estrada, S. Tikoo, A. Rosenberg, P. Kumar, M. Foldvari, In vivo cutaneous interferon-gamma gene delivery using novel dicationic (gemini) surfactant–plasmid complexes, J. Gene Med. 7 (2005) 1200–1214.
[30] K.H. Jennings, I.C.B. Marshall, M.J. Wilkinson, A. Kremer, A.J. Kirby, P. Camilleri, Aggregation properties of a novel class of cationic gemini surfactants correlate with their efficiency as gene transfection agents, Langmuir 18 (2002) 2426–2429.
[31] C.R. Dass, Lipoplex-mediated delivery of nucleic acids: factors affecting in vivo transfection, J. Mol. Med. 82 (2004) 579–591.
[32] A.M.S. Cardoso, H. Faneca, J.A.S. Almeida, A.A.C.C. Pais, E.F. Marques, M.C.P. de Lima, A.S. Jurado, Gemini surfactant dimethylene-1,2-bis(tetradecyldimethylammonium bromide)-based gene vectors: a biophysical approach to transfection efficiency, Biochim. Biophys. Acta 1808 (2011) 341–351.
[33] E. Fisicaro, C. Compari, E. Duce, G. Donofrio, B. Rózycka-Roszak, E. Woźniak, Biologically active bisquaternary ammonium chlorides: physico-chemical properties of long chain amphiphiles and their evaluation as non-viral vectors for gene delivery, Biochim. Biophys. Acta 1722 (2005) 224–233.
[34] T.C. Huang, H. Toraya, T.N. Blanton, Y. Wu, X-ray powder diffraction analysis of silver behenate, a possible low-angle diffraction standard, J. Appl. Crystallogr. 26 (1993) 180–184.
[35] N. Roveri, A. Bigi, P.P. Castellani, E. Foresti, M. Marchini, R. Strocchi, Study of rat tail tendon by x-ray diffraction and freeze-etching technics, Boll. Soc. Ital. Biol. Sper. 56 (1980) 953–959.
[36] D. Chapman, The polymorphism of glycerides, Chem. Rev. 62 (1962) 433–456.
[37] M. Kellens, W. Meeussen, H. Reynaers, Crystallization and phase transition studies of tripalmitin, Chem. Phys. Lipids 55 (1990) 163–178.
[38] J.O. Rädler, I. Koltover, T. Salditt, C.R. Safinya, Structure of DNA–cationic liposome complexes: DNA intercalation in multilamellar membranes in distinct interhelical packing regimes, Science 275 (1997) 810–814.
[39] I. Koltover, T. Salditt, C. Safinya, Phase diagram, stability, and overcharging of lamellar cationic lipid–DNA self-assembled complexes, Biophys. J. 77 (1999) 915–924.
[40] S. May, D. Harries, A. Ben-Shaul, The phase behavior of cationic lipid–DNA complexes, Biophys. J. 78 (2000) 1681–1697.
[41] T. Salditt, I. Koltover, J. Rädler, C. Safinya, Two-dimensional smectic ordering of linear DNA chains in self-assembled DNA–cationic liposome mixtures, Phys. Rev. Lett. 79 (1997) 2582–2585.
[42] D. Pozzi, H. Amenitsch, R. Caminiti, G. Caracciolo, How lipid hydration and temperature affect the structure of DC-Chol–DOPE/DNA lipoplexes, Chem. Phys. Lett. 422 (2006) 439–445.
[43] P. Balgavý, F. Devínsky, Cut-off effects in biological activities of surfactants, Adv. Colloid Interface Sci. 66 (1996) 23–63.
[44] G. Caracciolo, R. Caminiti, D. Pozzi, M. Friello, F. Boffi, A. Congiu Castellano, Self-assembly of cationic liposomes–DNA complexes: a structural and thermodynamic study by EDXD, Chem. Phys. Lett. 351 (2002) 222–228.
[45] J. Seelig, P.M. Macdonald, P.G. Scherer, Phospholipid head groups as sensors of electric charge in membranes, Biochemistry 26 (1987) 7535–7541.
[46] P.G. Scherer, J. Seelig, Electric charge effects on phospholipid headgroups phosphatidylcholine in mixtures with cationic and anionic amphiphiles, Biochemistry 28 (1989) 7720–7728.
[47] V. Matti, J. Säily, S.J. Ryhänen, J.M. Holopainen, S. Borocci, G. Mancini, P.K. Kinnunen, Characterization of mixed monolayers of phosphatidylcholine and a dicationic gemini surfactant SS-1 with a langmuir balance: effects of DNA, Biophys. J. 81 (2001) 2135–2143.
[48] S.J. Ryhänen, M.J. Säily, T. Paukku, S. Borocci, G. Mancini, J.M. Holopainen, P.K.J. Kinnunen, Surface charge density determines the efficiency of cationic gemini surfactant based lipofection, Biophys. J. 84 (2003) 578–587.
[49] L. Zhang, T.A. Spurlin, A.A. Gewirth, S. Granick, Electrostatic stitching in gel-phase supported phospholipid bilayers, J. Phys. Chem. B 110 (2006) 33–35.
[50] S. Bandyopadhyay, M. Tarek, M.L. Klein, Molecular dynamics study of a lipid −DNA complex, J. Phys. Chem. B 103 (1999) 10075–10080.
[51] A.A. Gurtovenko, M. Patra, M. Karttunen, I. Vattulainen, Cationic DMPC/DMTAP lipid bilayers: molecular dynamics study, Biophys. J. 86 (2004) 3461–3472.
[52] G. Caracciolo, D. Pozzi, R. Caminiti, C. Marchini, M. Montani, A. Amici, H. Amenitsch, Transfection efficiency boost by designer multicomponent lipoplexes, Biochim. Biophys. Acta 1768 (2007) 2280–2292.
[53] J. Mou, D.M. Czajkowsky, Y. Zhang, Z. Shao, High-resolution atomic-force microscopy of DNA: the pitch of the double helix, FEBS Lett. 371 (1995) 279–282.
[54] S. May, A. Ben-Shaul, Modeling of cationic lipid–DNA complexes, Curr. Med. Chem. 11 (2004) 151–167.
[55] J. Sujatha, A.K. Mishra, Effect of ionic and neutral surfactants on the properties of phospholipid vesicles: investigation using fluorescent probes, J. Photochem. Photobiol. A 104 (1997) 173–178.
[56] I. Koltover, T. Salditt, J.O. Rädler, C.R. Safinya, An inverted hexagonal phase of cationic liposome–DNA complexes related to DNA release and delivery, Science 281 (1998) 78–81.
[57] R. Podgornik, D.C. Rau, V.A. Parsegian, Parametrization of direct and soft steric-undulatory forces between DNA double helical polyelectrolytes in solutions of several different anions and cations, Biophys. J. 66 (1994) 962–971.